BJR

https://doi.org/10.1259/bjr.20180126

Received: 31 January 2018 | Revised: 24 April 2018 | Accepted: 25 April 2018

Cite this article as:
Cunha GM, Glaser KJ, Bergman A, Luz RP, de Figueiredo EH, Lobo Lopes FPP. Feasibility and agreement of stiffness measurements using gradient-echo and spin-echo MR elastography sequences in unselected patients undergoing liver MRI. *Br J Radiol* 2018; **91**: 20180126.

FULL PAPER

Feasibility and agreement of stiffness measurements using gradient-echo and spin-echo MR elastography sequences in unselected patients undergoing liver MRI

[1]GUILHERME MOURA CUNHA, MD, [2]KEVIN J GLASER, PhD, [3]ANKE BERGMAN, PhD, [4]RODRIGO P LUZ, MD, [5]EDUARDO H DE FIGUEIREDO, B.Eng. and [1,6]FLAVIA PAIVA PROENÇA LOBO LOPES, MD, PhD

[1]MRI Department, Clínica de Diagnóstico por Imagem CDPI-DASA, Rio de Janeiro, Brazil
[2]Department of Radiology, Mayo Clinic, Rochester, MN, USA
[3]Programa de Carcinogênese Molecular, Instituto Nacional de Câncer (INCA), Rio de Janeiro, Brazil
[4]Hepatology, Universidade Federal do Rio De Janeiro, UFRJ, Cidade Universitária, Rio de Janeiro, Brazil
[5]MR Advanced Applications-Research , GE Healthcare, Latin America , São Paulo, Brazil
[6]Radiology Department, School of Medicine, Universidade Federal do Rio de Janeiro UFRJ, Rio de Janeiro, Brazil

Address correspondence to: Dr Guilherme Moura Cunha
E-mail: *mouracunha@hotmail.com; mouracunha@gmail.com*

Objective: To evaluate the agreement of three MR elastography (MRE) sequences in patients undergoing liver MRI for clinical care.
Methods: A cross-sectional retrospective study was performed with 223 patients referred for liver MRI, including 12 patients with liver iron overload. Data obtained with spin-echo (SE) and gradient-echo (GRE) MRE sequences were compared. Multiple linear regression adjusted for the presence of liver fat was also performed to assess the correlation between fat infiltration and stiffness measurements results. Agreement between two SE sequences was assessed in patients with liver iron overload.
Results: We found strong correlation between the GRE sequence and two SE sequences. Spearman's correlation coefficients between the GRE, SE, and SE-EPI MRE sequences in patients with liver R2* <75Hz were 0.74, 0.81, and 0.80. GRE-MRE failed in patients with liver R2* > 75 Hz. In this subgroup, the correlation coefficient between both SE-MRE sequences was 0.97. Liver fat did not interfere with the results.
Conclusion: In clinical setting, there is a high correlation between the GRE and SE MRE stiffness measurements, independently of the degree of liver fat infiltration measured by PDFF. A strong correlation between SE-MRE sequences is found even in patients with iron overload.
Advances in knowledge: Our study addresses liver iron and fat content simultaneously to describing the technical feasibility and correlation between different MRE sequences in consecutive unselected patients refereed for liver MRI. EPI SE-MRE should be considered an optimal alternative to assess liver fibrosis in patients in whom GRE-MRE failures, such as iron-overloaded, in pediatric, elderly, or severely ill populations.

INTRODUCTION

Liver fibrosis can occur secondary to chronic hepatocellular injury, related to multiple causes, the most common being fat infiltration, chronic viral infections, and alcohol abuse. Less prevalent causes include liver iron overload. Higher liver iron uptake can also be a consequence of chronic liver diseases, which ultimately contributes to hepatocellular damage and carcinogenesis.[1,2] Although liver biopsy is the current gold-standard for the diagnosis and staging of liver iron overload, liver fat deposition, and fibrosis, it has limitations, most related to sampling errors and only moderate interreader agreement.[3–6] Percutaneous liver biopsy is also an invasive procedure with potential risks and unsuitable for consecutive routine follow-up assessment.[4] To address liver pathologies non-invasively, novel imaging quantification techniques have been the focus of extensive research. T_2* and R2* calculations using conventional MRI relaxometry can indirect determine liver iron content. Relaxometry sequences such as IDEAL-IQ® (Iterative Decomposition of water and fat with Echo Asymmetry and Least-squares estimation) uses multipeak fat corrections instead of magnitude-only data fitting providing rectification for inaccurate results often caused by the presence concomitant liver fat deposition. By assessing the liver fat content for bias correction, IDEAL-IQ® provides for the same acquisition proton-density fat fraction images with corresponding quantification parametric maps.[3,7] MR elastography (MRE) is an imaging

technique that noninvasively assesses the mechanical properties of organs and tissues and can indirectly measure tissue stiffness. In the liver, stiffness tends to increase with collagen deposition and MRE results accurately correlates with the histology fibrosis grades.[8,9] Different MRE techniques are applicable and provided by different vendors. The most widely available commercial MRE technique is based on gradient-echo (GRE) sequences. GRE MRE has been shown to be a very precise tool to evaluate liver fibrosis in large cohort studies and meta-analysis.[10–13] However, in the presence of iron overload, the conventional GRE MRE technique fails due to T_2* dephasing and signal loss from the liver.[14] GRE MRE sequences can also show poor results in patients with larger body habitus due to signal loss and limited encoding of the shear waves in the deeper areas of the liver.[15] As chronic liver disease is often associated with liver iron overload and obesity, radiologists should be aware of the potential limitations of GRE-based techniques and how other protocols using spin-echo (SE) sequences can potentially improve results. SE-based MRE sequences are intrinsically insensitive to T_2* susceptibility due to the presence of a refocusing pulse and low TE value. Nevertheless, SE acquisitions can be longer than the equivalent GRE acquisitions, needing longer breath-holds or serial breath-holds in a short interval, a major limitation especially in pediatric, elderly, or severely ill populations.[15] Echo-planar imaging (EPI) is a fast MRI technique that, by obtaining all spatial-encoding information in a single radio-frequency (RF) pulse, allows more rapid acquisition times with less motion artifacts.[16] SE MRE acquisitions performed using EPI have a rapid readout, hence, faster acquisition times with fewer or shorter breath-holds required.[14,16]

Either for iron, fat and liver fibrosis assessment, available data in the literature have shown a high accuracy of non-invasive MRI quantification techniques in correlation to histology as a reference standard.[9–11,17–20] This makes a sufficient solid ground to justify the absence of an independent invasive reference standard such as liver biopsy in chronic liver disease-related studies.[21,22]

This study was designed to evaluate the agreement of three MRE sequences (one GRE and two SE) in patients undergoing liver MRI for clinical care. Multiple linear regression adjusted for the presence of liver fat was performed to assess the correlation between fat infiltration and stiffness measurements results. As a secondary aim, we tested the agreement between the two SE sequences in patients whom the GRE sequence has failed due to the presence of liver iron overload, as an alternative for liver fibrosis detection in this population.

METHODS AND MATERIALS

This cross-sectional retrospective study was designed using data from patients referred for liver MRI as part of their clinical care, either for diffuse liver disease or focal liver lesions, from December 2016 to December 2017. The institutional review board approved the study, and the requirement to obtain written informed consent was waived for retrospective review of data from patients who underwent clinically indicated MRE.

Subjects

Of a total of 225 patients, two patients were excluded from the analysis due to significant motion artefact image degradation. A total of 223 patients met the inclusion criteria as follows: (i) had liver R2* and proton-density fat fraction estimations determined by a three-dimensional volumetric imaging sequence (IDEAL-IQ®), (ii) acquisition of the MRE pulse sequences in our clinical protocol with at least two of the sequences having the post-processed data available for shear wave stiffness measurements.

Imaging technique

All patients were scanned in supine position in a 1.5T magnet (450W, GE, Milwaukee, WI). Imaging protocol consisted of two main image blocks. First, a standard abdomen MRI protocol (axial GRE T_1 weighted in-phase/opposed-phase, T_2 weighted SSFSE, diffusion weighted imaging (b = 50, 750), pre- and post-intravenous gadolinium administration fat-saturated T_1 weighted spoiled-GRE images. Second, quantitative MR images as follows: (i) Multiple-echo spoiled-GRE for PDFF and R2* estimation using IDEAL-IQ®, (ii) MRE images using three different acquisition sequences: (1) commercially available 2D GRE MRE sequence (GRE-MRE), (2) SE MRE sequence (non-EPI), and (3) SE-EPI MRE sequence.

PDFF and R2* measurements

PDFF and R2* values were obtained using a multipoint Dixon technique (IDEAL-IQ®) with six echoes acquired with a low flip angle and a multipeak fat model to limit T_1- and fat-related biases. Volumetric acquisition with 10 mm slices covering the whole liver were performed during a single breath hold to generate PDFF and R2* parametric maps. Measurements were performed by one reader (abdominal radiologist with 10 years of experience). To maintain consistency, a 5 cm^2 round region of interest (ROI) was placed over the right liver lobe, as central as possible aiming for the transition of segments V, VI, VII, and VIII, in all cases, according to anatomical landmarks, avoiding major liver vessels, focal lesions, and vicinity to liver margins, fat or gas. We categorized liver fat deposition based on PDFF measurements according to cut-offs previously described in the literature[5,7,20] as follows: 0 = no steatosis (PDFF: <5.0%), 1 = mild fat deposition (PDFF: 5.1 to 15.0%), 2 = moderate fat deposition (PDFF: 15.1–30.0, %), 3 = severe fat deposition (PDFF: >30.1%). For this study, we considered R2* values higher than 75 Hz at 1.5T as a cut-off value to determine abnormal liver iron content. This threshold was defined based on the observation that most of the GRE-MRE acquisitions failed in patients with R2* values higher than 75 Hz and being a sufficiently high value to assure iron overload despite variations reported in the literature.

MRE stiffness measurements

All patients were scanned using three different MRE sequences in the same examination, as follows: (i) a commercially available 2D GRE MRE sequence [MR-Touch® GE, Milwaukee, WI] (named "GRE-MRE"), (ii) a SE (non-EPI) MRE sequence (named "SE-MRE"), and (iii) a SE-EPI MRE sequence (named "EPI-MRE"). MRE sequence parameters are provided in Table 1. Total scan times for the three MRE sequences were 55, 69, and

Table 1. Imaging parameters for IDEAL IQ® and the three MRE sequences

	IDEAL IQ®	2D GRE MRE (MR Touch®)	2D SE MRE	2D SE (EPI) MRE
FOV (cm)	40.0	42.0	42.0	42.0
Slice thickness (mm)	10	8.0	8.0	8.0
Slice spacing (mm)	.	2.0	2.0	2.0
Number of slices	N/A	4	4	4
Matrix	128 × 128	256 × 64	80 × 80	128 × 64
Phase FOV	0.8	1.0	1.0	0.8
NEX	0.5	1.0	1.0	0.75
TR (ms)	11.9	50.0	200.0	1000.0
TE (ms)	4.3	21.8	10.2	18.6
Parallel Imaging	1.0	1.0	1.0	2.0
Receiver bandwith (Hz)	100.0	31.25	62.5	250.0
MEG direction	N/A	MEG Direction Z	MEG Direction Z	MEG Direction Z
Total acquisition time (s)	17	55	69	30
Number of breath-holds	1	4	5	2

NEX, Number of excitations; TR, Repetition Time; TE, Echo Time; MEG, Motion Encoding Gradient; FOV, field of view; GRE, gradient-echo; MRE, MR elastography; SE, spin-echo.

30 s, respectively. All sequences were acquired using appropriate concatenations to assure a maximum breath-hold time of ≈ 15 s. Therefore, the number of breath-holds for each of the used sequences were 4, 5, and 2. For assessing liver fibrosis, the same reader drew ROIs over the MRE-generated magnitude images. Two 5 cm^2, round ROIs were placed over the right liver lobe at the same position in all sequences (copy-pasted), also avoiding large vessels, focal lesions, the gallbladder or the region immediately below the driver. During ROIs positioning to assess liver fibrosis the reader was blind to PDFF and R2* parametric maps so as not to be biased by its results. ROIs were carefully placed within regions of high confidence indicated by the reconstruction algorithm over the parametric maps where the propagating waves had both good amplitude and a clear dominant propagation direction. Overall, liver stiffness was calculated by averaging the mean shear stiffness values from both ROIs in each individual patient. Five fibrosis grades were defined according to previously published data in the literature as follows: F0 (<2.9 kPa), F1 (3.0–3.5 kPa), F2 (3.6–4.2 kPa), F3 (4.3–5.1 kPa), F4 (>5.1 kPa).[12,23] However, we have also divided the stiffness results into three categories for clinical significance of liver fibrosis. Patients with liver stiffness of <2.9 kPa where scored as no fibrosis; patients with stiffness values between 3.0–4.2 kPa were scored as mild to moderate fibrosis; and patients with stiffness values higher than 4.3 kPa were scored as advanced fibrosis.

Statistical analysis

The statistical software SPSS (SPSS Inc., Chicago, IL) was used for all analysis. For the descriptive analysis of the population, central tendency measurements were performed for the quantitative variables, and absolute and relative frequency distributions for the qualitative variables. Liver stiffness values obtained with all three MRE sequences were compared using the Spearman's correlation test. GRE-MRE results were correlated to values obtained with both SE sequences in patients with liver R2* values < 75 Hz (no iron overload). The two SE sequences were correlated in this same cohort of patients, as well as, in the cohort of patients with liver R2* values higher than 75 Hz (iron overload). Multiple linear regression adjusted for the presence of liver fat was also performed to assess the correlation between fat infiltration and stiffness measurements results. p values < 0.05 were considered as statistically significant.

RESULTS

A total of 223 patients were included in the analysis. Age range was 26 to 85 years old (mean: 60.5 years) and the sex distribution was 133 male patients and 90 females. All patients were referred for clinical indicated MRI due to a variety of conditions, including diffuse and focal liver disease, such as NAFLD, liver iron-overload, chronic hepatitis of different etiologies, benign and malignant liver nodules etc. Distribution of liver steatosis grades based on MRI-PDFF results in the 223 patients was: 0 = 64 patients, 1 = 95 patients, 2 = 47 patients and 3 = 17 patients. 12 patients had abnormally elevated liver iron content defined as R2* values > 75 Hz. In these patients GRE-MRE failed to provide results due to very low signal-to-noise ratio (SNR) to allow image reconstruction or failure to indicate a high-confidence area over the elastogram maps from which to perform our measurements (Figure 1). In five patients with R2* values lower than 75 Hz GRE-MRE also failed due to poor shear waves displacement visualization secondary to low SNR over the liver area related to other causes than iron-overload such as obesity and respiratory motion artifacts. Among these patients, three had body mass indices higher than 39.7 Kg m^{-2} and two could not hold an apnea for longer than 8 s.

Liver stiffness using the GRE-MRE sequence was evaluated in a total of 206 patients with the following fibrosis grade distribution:

Figure 1. (a) A 36-year-old male with hereditary hemochromatosis (HFE gene: C282y/C282y). IDEAL-IQ® R2* parametric map shows diffuse high signal intensity in the liver indicating high liver iron content. R2* = 355 Hz. Same patient (b, c): Elastographic images for whom the commercial GRE-MRE measurement failed. The significant signal loss and low SNR over the liver area secondary to the presence of iron causes poor image quality and low confidence in the stiffness estimates. (b) Wave image: The presence of iron causes significant signal loss over the liver area and poor shear waves displacement visualization leading to invalid shear stiffness estimates. (c) Elastogram: SNR is below a value that permits image reconstruction over the liver area resulting in a distorted image. (d, e) Same patient, successful SE-EPI-MRE sequence elastographic images: Despite the high iron liver content, the SNR is high enough to provide valid stiffness measurements. (d) Wave image: High SNR permits good visualization of shear waves. (e) SE-EPI-MRE parametric map (color elastogram map)—High SNR permits shear stiffness to be successfully calculated for parametric map reconstruction. EPI, echo-planar imaging; GRE, gradient-echo; MRE, MR elastography; SE, spin-echo; SNR, signal-to-noise ratio.

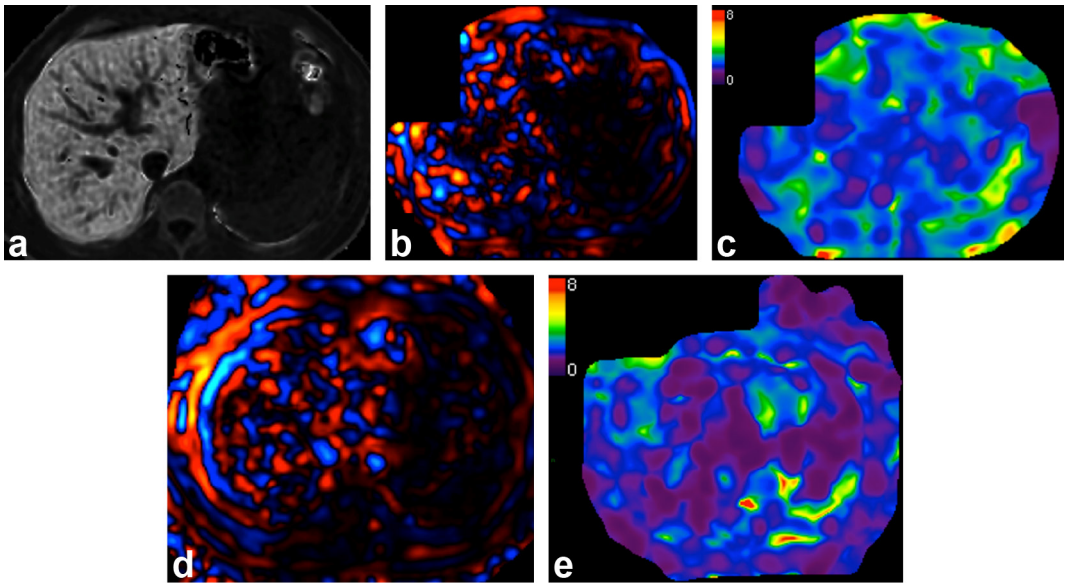

F0 (<2.9 kPa)—158 patients, F1 (3.0–3.5 kPa)—14 patients, F2 (3.6–4.2 kPa)—10 patients, F3 (4.3–5.0 kPa)—7 patients, F4 (>5.1 kPa)—16 patients. When stratified into mild to moderate *vs* advanced liver fibrosis, the distribution was: 158 patients with no fibrosis (F0), 24 patients with mild to moderate fibrosis, and 23 patients with advanced fibrosis (F3/F4). Both SE sequences had enough SNR in all 223 patients to successfully provide magnitude images and parametric stiffness maps showing measurable areas with a confidence index higher than 95% (Figure 2). Using the mild to moderate *vs* advanced fibrosis stratification, distribution using SE-MRE was: 165 patients with no fibrosis (F0), 23 patients with mild to moderate fibrosis (F1/F2), and 23 patients with advanced liver fibrosis (F3/F4). Distribution of the fibrosis grade for EPI-MRE using the same criteria was: 157 patients with no fibrosis (F0), 25 patients with mild to moderate fibrosis (F1/F2), and 28 patients with advanced liver fibrosis (F3/F4). Regarding stiffness values in Kilopascal using the three different sequences, the median was 2.3 kPa (min. 1.2 kPa – max. 13.1 kPa) for GRE-MRE, 2.2 kPa (min. 1.3 kPa – max. 13.7 kPa) for EPI-MRE, and 2.1 kPa (min. 1.0 kPa – max.11.7 kPa) for SE-MRE. We found excellent correlation between the GRE-MRE sequence and both SE sequences in patients with R2* < 75 Hz. Spearman's correlation coefficients between the GRE-MRE and SE-MRE sequences, the GRE-MRE and EPI-MRE, and the two SE-MRE sequences in this subset of patients were 0.74, 0.81, and 0.80, respectively. In the subset of patients with R2* values higher than 75 Hz, the correlation between the SE sequences (SE-MRE and MRE-EPI) was 0.97 (Figure 3). Correlation results were not interfered by the presence of liver fat infiltration. Linear regression analysis and multiple linear regression analysis adjusted for the presence of liver fat for comparison of stiffness results obtained by GRE-MRE *vs* SE-MRE, GRE-MRE *vs* EPI-MRE, SE-MRE *vs* EPI-MRE are shown in Figure 4.

DISCUSSION

MRE has established itself as a noninvasive diagnostic tool for the assessment of hepatic fibrosis. Our results show strong correlation between different MRE sequences in clinical indicated liver MRI in a variety of conditions including liver fat infiltration and iron overload. Most widely commercial available implementation of the technique uses a fast GRE-based 2D MRE sequence. While a convenient and robust method, it has limitations related to lower SNR, longer scanning times and failure in patients with liver iron overload. SE sequences can potentially overcome some of these limitations by providing higher SNR and intrinsically insensitive to T_2* susceptibility effects. At our institution, all patients referred for liver MRI as part of clinical care are evaluated for the presence of iron overload, liver fat deposition and liver fibrosis, the latter performed by using three different MRE sequences. We conducted a study to evaluate the technical feasibility and agreement between these sequences (a commercial available GRE-MRE sequence and two SE-based MRE sequences) for liver stiffness assessment in patients undergoing clinically indicated liver MRI for various conditions. For routine

Figure 2. A 44-year-old male, ferritin > 2800 ng/dL. (a) IDEAL-IQ R2* parametric map shows diffuse high signal intensity related to high iron content. Liver R2*= 110 Hz. (b–d) Elastograms color maps of estimated stiffness with a checkerboard mask covering areas that have a confidence index lower than 0.95 and should be avoided when drawing an ROI to report the stiffness. Success rates and image quality are higher in SE sequences, despite the high iron liver content. (b) GRE-MRE color elastogram map shows significant low SNR over the liver resulting in distorted images and no valid areas within the algorithm generated confidence interval (0.95). (c, d) – SE MRE and Spin-echo EPI-MRE sequences parametric maps (elastogram) - High SNR permits shear stiffness to be successfully calculated for parametric map reconstruction and values are within the algorithm generated confidence interval (0.95). ROIs should be drawn within this areas for stiffness measurements. EPI, echo-planar imaging; GRE, gradient-echo; MRE, MR elastography; ROI, region of interest; SE, spin-echo; SNR, signal-to-noise ratio.

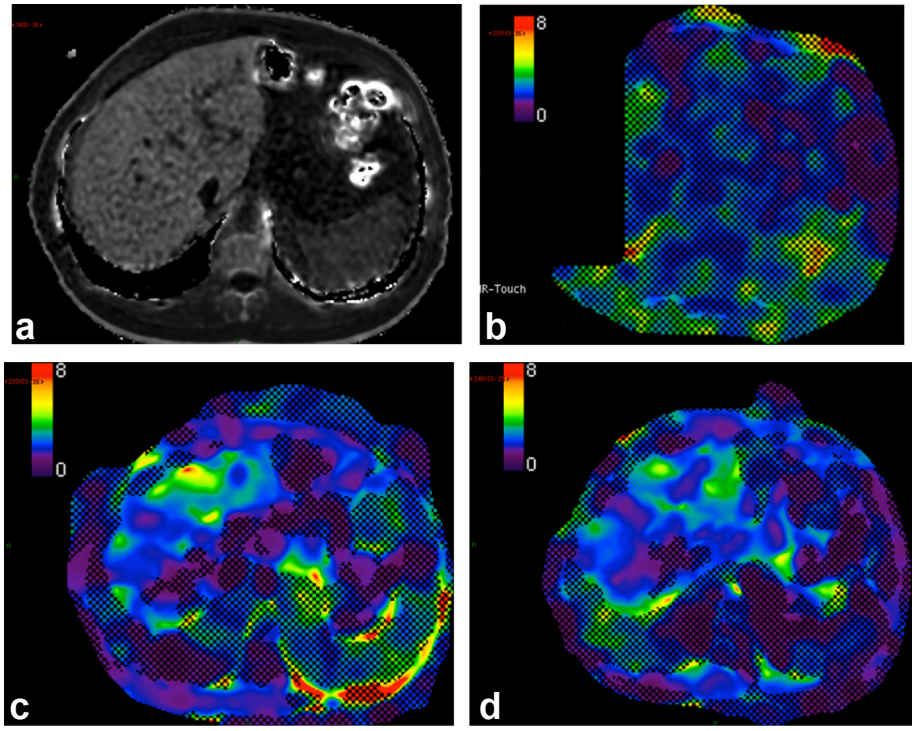

clinical examinations, threshold values for liver iron quantification are often extrapolated from the literature without individual calibrations, leading to variability of adopted threshold of T_2* and R2* values. For this study, we considered R2* values higher than 75 Hz at 1.5 Tesla as a cut-off value to determine liver iron overload. Although we are aware that much lower thresholds have been used and previously described,[24,25] we chose to consider a higher value to guarantee a consistent cut-off that would undoubtedly be related to the presence of iron overload. Also, we observed that the GRE-MRE acquisitions failed when R2* values were higher than 75 Hz due to significant signal loss. Regarding liver stiffness and fibrosis grading, there is some variety of thresholds in the literature, as other cut-off values have also been adopted in different studies.[26,27] We hypothesize that these discrepancies may be related to the differences in the amount of collagen deposition and inflammatory grade within each fibrosis stage across different liver disease etiologies. We have based our analysis on the values described by Chang et al and Srinivasa et al.[12,23] Both works were not limited to a specific condition or population, therefore, more suitable to the diversity of our population.[23] However, we also stratified the results in three categories of liver fibrosis, based on clinical significance. We believe that due to some variations in the literature regarding the exact cut-off values for any given fibrosis grade, the latter categorization may be more suitable and have stronger implication for the unselected sort of our population. To the best of our knowledge, no previous work has addressed simultaneously liver iron and fat quantification techniques and different MRE sequences in an unselected population undergoing clinical indicated MRI. Mariappan et al has tested two similar SE-MRE sequences in comparison to GRE-MRE in a clinical setting, however, not addressing liver iron and fat quantification sequences.[14] Some of the largest meta-analysis of individual participant data have either selected patients with a prior known diagnosis of chronic liver disease or other specific populations.[26,28] When selecting only patients with known chronic liver disease the mean liver stiffness across the cohort tends to be higher than the average values in the general population. Therefore, individuals with unknown chronic liver disease and/or who present with only subtle liver stiffness alterations, tends to be not addressed in these results. We found high correlation between all three MRE sequences in accordance with previous studies in the literature in different clinical scenarios.[14,15,29,30] The presence of fat and various degrees of liver fat deposition did not interfere with the correlation between MRE sequences. In patient with R2* < 75 Hz correlations were 0.80 between GRE-MRE and EPI-MRE and 0.89 between GRE-MRE and SE-MRE. We found strong correlations between SE sequences (EPI-MRE *vs* SE-MRE) (0.98 and

Figure 3. Correlation between liver stiffness measurements obtained using the GRE and SE MRE sequences in patients without liver iron-overload (R2* < 75Hz): (a) GRE-MRE and SE-MRE, (b) GRE-MRE and SE-EPI MRE, and (c) both SE MRE sequences. (d) Correlation between SE MRE sequences in patients with elevated liver iron content (R2* > 75Hz). EPI, echo-planar imaging; GRE, gradient-echo; MRE, MR elastography; SE, spin-echo.

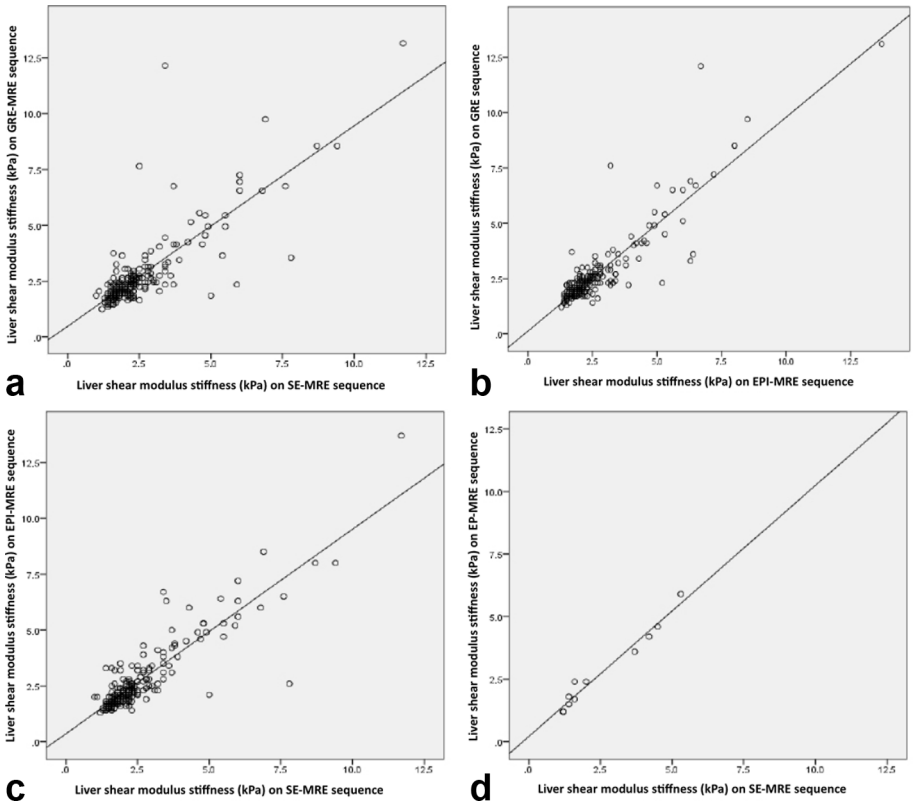

0.88, respectively) in patients with and without iron overload. In our study, 12 patients with R2* values higher than 75 Hz could not have their liver stiffness determined using GRE-MRE due to significant signal loss related to susceptibility. In other five patients GRE-MRE failed due to low SNR of causes other than liver iron overload. In this study we used a standard commercial available GRE-MRE sequence provided by the scanner manufacturer (MR-Touch® GE, Milwaukee, WI). We did not change any of the preset parameters so to evaluate the sequence's strengths and limitations, not based on theoretical research, but focusing on daily practice clinical routine. Using a mechanical vibration frequency of 60 Hz and same frequency motion encoding gradients, the preset TE value in this sequence was 21.8 ms. This is a sufficiently long TE to result in lengthy acquisition times, as well as, to disserve tissues with short T_2 values or areas with high susceptibility leading to significant signal decay.[31] Hence, when signal decay was more pronounced due to iron overload, the SNR was very poor on GRE-MRE images. In comparison, with SE MRE acquisitions no failure was observed in all patients included in our analysis. Although GRE-MRE and SE MRE show equally good diagnostic performance in staging liver fibrosis, success rates and image quality have been shown to be

Figure 4. Tables show linear regression analysis and multiple linear regression analysis adjusted for the presence of liver fat for comparison of stiffness results obtained by (a) GRE-MRE and SE MRE sequences and (b) SE-MRE and EPI-MRE in patients with R2* < 75Hz. (c) Rgression analysis and multiple linear regression analysis adjusted for the presence of liver fat for comparison of SE MRE sequences in patients with R2* > 75Hz. EPI, echo-planar imaging; GRE, gradient-echo; MRE, MR elastography; SE, spin-echo.

a

	SE MRE						SE-EPI MRE					
GRE-MRE	Simple			Adjusted for Liver Fat			Simple			Adjusted for Liver Fat		
	B	C.I.	p-value	B	C.I.	p-Value	B	C.I.	p-value	B	C.I.	p-Value
	0.71	0.64 - 0.79	<0.001	0.71	0.64 - 0.79	<0.001	0.82	0.76 - 0.88	<0.001	0.82	0.76 - 0.88	<0.001

b

	SE MRE					
SE-EPI MRE	Simple			Adjusted for Liver Fat		
	B	C.I.	p-value	B	C.I.	p-Value
	0.85	0.79 - 0.91	<0.001	0.85	0.79 - 0.92	<0.001

c

	SE MRE					
SE-EPI MRE	Simple			Adjusted for Liver Fat		
	B	C.I.	p-value	B	C.I.	p-Value
	0.85	0.79 - 0.91	<0.001	0.85	0.79 - 0.92	<0.001

significantly higher in SE sequences.[32,33] Our higher success rate of the SE MRE is also in accordance to success rates previously described in the literature.[30–34] This relates to the higher susceptibility and lower SNR of GRE sequences. Susceptibility issues are more pronounced at higher field strength and we hypothesize that at 3.0 T failure rates would have been even higher using GRE-MRE including patients with mild iron overload and lower R2* values.[34,35] An alternative to reduce signal loss and susceptibility problems encountered with standard GRE-MRE sequences is to apply a fractional encoding approach using lower and in-phase TE values, which results in less susceptibility and higher SNR for image acquisition.[31,36] However, this could only partially resolve the issue, as high susceptibility and severe iron overload could still represent a problem. The use of SE MRE sequences in patients with liver iron overload is then still preferred at 3T.[27,33,34] We found a high correlation between SE-MRE and EPI-MRE stiffness results either in patients with and without iron overload. SE-based EPI-MRE sequences can be even more advantageous in comparison with GRE-MRE. First, as mentioned, it is inherently insensitive to T_2* signal decay effect. Secondly, SE EPI-MRE provides faster acquisitions often leading to shorter breath-holds needed, which can be quite advantageous in patients showing difficulties in performing longer apnea. One potential disadvantage of EPI sequences are off-resonance artifacts related to low bandwidth in the phase-encoding direction that results in geometric distortions.[31,37] However, we did not experience major SE-EPI MRE image degradation that could be related to this phenomenon.

As liver MRE continues to be established as a reliable technique for assessing fibrosis noninvasively, it should be offered to all patients with chronic liver disease. This should include patients with liver iron overload and severely ill individuals with difficulties in performing long breath-holds for image acquisition. Radiologists, hepatologists and other referring physicians involved in the care of chronic liver diseases should be fully aware of the applicability of these sequences in evaluating fibrosis as alternatives to the most widely available GRE-MRE sequences. Our study has some limitations. First, we did not perform an invasive assessment of the liver fat and iron content, neither fibrosis grade as a standard of reference. We understand that the extensive data available in the literature describing the use of MRI as a reliable and accurate tool to noninvasively assess these conditions is a sufficiently strong foundation on which to base our analysis. Another limitation of our study is the small number of patients with liver iron overload among the total number of included individuals, which limits the analysis regarding this specific condition.

In conclusion, we found a high correlation between the GRE and SE MRE stiffness measurements. Strong correlation between the three MRE sequences were seen independently of the degree of liver fat deposition measured by PDFF. Correlations between the EPI and non-EPI SE MRE sequences in patients with iron overload was also high. As GRE-MRE sequences are subject to higher failure rates due to high iron liver content and other limitations, SE-MRE sequences should be considered as an adequate alternative to assess liver fibrosis. Also, considering the advantages of faster acquisition times, SE-based EPI-MRE sequences can be a more suitable approach to assess liver fibrosis in pediatric, elderly, or severely ill populations.

ACKNOWLEDGEMENTS

We acknowledge Dr Richard L. Ehman MD., as well as, Scott Kruse from the Mayo Clinic Department of Radiology who provided us with technical details and better understanding regarding all noncommercial MRE sequences. Also, ours MRI technicians (Carlos Eduardo Lima Dantas and Poliana Teixeira Castro) who were directly involved in this project.

CONFLICTS INTEREST

Author Kevin J. Glaser and his department are supported in part by NIH grant EB001981. Nevertheless, this particular work did not receive any direct support by this grant. This author and Mayo Clinic have intellectual property rights and a financial interest in MR elastography technology. Eduardo Figueiredo is a GE Healthcare employee. All other authors involved in this work declare that they have no conflict of interest.

FUNDING

This study was performed without any external funding. All data was retrospectively collected from patients who underwent clinically indicated MRI at our institution and authors received no funding regarding their work in this manuscript.

ETHICS APPROVAL

All procedures performed in studies involving human participants were in accordance with the ethical standards of the institutional and/or national research committee and with the 1964 Helsinki declaration and its later amendments or comparable ethical standards.

INFORMED CONSENT

The requirement to obtain written informed consent was waived for retrospective review of data from patients who underwent clinically indicated MRE.

REFERENCES

1. Runge JH, Akkerman EM, Troelstra MA, Nederveen AJ, Beuers U, Stoker J. Comparison of clinical MRI liver iron content measurements using signal intensity ratios, R_2 and R_2*. *Abdom Radiol* 2016; **41**: 2123–31. doi: https://doi.org/10.1007/s00261-016-0831-7
2. Mueller J, Raisi H, Rausch V, Peccerella T, Simons D, Ziener CH, et al. Sensitive and non-invasive assessment of hepatocellular iron using a novel room-temperature susceptometer. *J Hepatol* 2017; **67**: 535–42. doi: https://doi.org/10.1016/j.jhep.2017.04.019

3. Pournik O, Alavian SM, Ghalichi L, Seifizarei B, Mehrnoush L, Aslani A, et al. Inter-observer and Intra-observer agreement in pathological evaluation of non-alcoholic fatty liver disease suspected liver biopsies. *Hepat Mon* 2014; **14**: e15167. doi: https://doi.org/10.5812/hepatmon.15167
4. Sirlin CB, Reeder SB. Magnetic resonance imaging quantification of liver iron. *Magn Reson Imaging Clin N Am* 2010; **18**: 359–81. doi: https://doi.org/10.1016/j.mric.2010.08.014
5. Jung ES, Lee K, Yu E, Kang YK, Cho MY, Kim JM, et al. Interobserver agreement on pathologic features of liver biopsy tissue in patients with nonalcoholic fatty liver disease. *J Pathol Transl Med* 2016; **50**: 190–6. doi: https://doi.org/10.4132/jptm.2016.03.01
6. German AL, Fleming K, Kaye P, Davies S, Goldin R, Hubscher SG, et al. Can reference images improve interobserver agreement in reporting liver fibrosis? *J Clin Pathol* 2018; **71**: 368–71. doi: https://doi.org/10.1136/jclinpath-2017-204760
7. Reeder SB, Sirlin CB. Quantification of liver fat with magnetic resonance imaging. *Magn Reson Imaging Clin N Am* 2010; **18**: 337–57. doi: https://doi.org/10.1016/j.mric.2010.08.013
8. Venkatesh SK, Ehman RL. Magnetic resonance elastography of liver. *Magn Reson Imaging Clin N Am* 2014; **22**: 433–46. doi: https://doi.org/10.1016/j.mric.2014.05.001
9. Yin M, Glaser KJ, Talwalkar JA, Chen J, Manduca A, Ehman RL. Hepatic MR elastography: clinical performance in a series of 1377 consecutive examinations. *Radiology* 2016; **278**: 114–24. doi: https://doi.org/10.1148/radiol.2015142141
10. Loomba R, Wolfson T, Ang B, Hooker J, Behling C, Peterson M, et al. Magnetic resonance elastography predicts advanced fibrosis in patients with nonalcoholic fatty liver disease: a prospective study. *Hepatology* 2014; **60**: 1920–8. doi: https://doi.org/10.1002/hep.27362
11. Shi Y, Guo Q, Xia F, Dzyubak B, Glaser KJ, Li Q, et al. MR elastography for the assessment of hepatic fibrosis in patients with chronic hepatitis B infection: does histologic necroinflammation influence the measurement of hepatic stiffness? *Radiology* 2014; **273**: 88–98. doi: https://doi.org/10.1148/radiol.14132592
12. Chang W, Lee JM, Yoon JH, Han JK, Choi BI, Yoon JH, et al. Liver fibrosis staging with MR elastography: comparison of diagnostic performance between patients with chronic hepatitis B and those with other etiologic causes. *Radiology* 2016; **280**: 88–97. doi: https://doi.org/10.1148/radiol.2016150397
13. Ichikawa S, Motosugi U, Ichikawa T, Sano K, Morisaka H, Enomoto N, et al. Magnetic resonance elastography for staging liver fibrosis in chronic hepatitis C. *Magn Reson Med Sci* 2012; **11**: 291–7. doi: https://doi.org/10.2463/mrms.11.291
14. Mariappan YK, Dzyubak B, Glaser KJ, Venkatesh SK, Sirlin CB, Hooker J, et al. Application of modified spin-echo-based sequences for hepatic MR elastography: evaluation, comparison with the conventional gradient-echo sequence, and preliminary clinical experience. *Radiology* 2017; **282**: 390–8. doi: https://doi.org/10.1148/radiol.2016160153
15. Serai SD, Dillman JR, Trout AT. Spin-echo echo-planar imaging MR elastography versus gradient-echo MR elastography for assessment of liver stiffness in children and young adults suspected of having liver disease. *Radiology* 2017; **282**: 761–70. doi: https://doi.org/10.1148/radiol.2016160589
16. DeLaPaz RL. Echo-planar imaging. *Radiographics* 1994; **14**: 1045–58. doi: https://doi.org/10.1148/radiographics.14.5.7991813
17. Garbowski MW, Carpenter J-P, Smith G, Roughton M, Alam MH, He T, et al. Biopsy-based calibration of T2* magnetic resonance for estimation of liver iron concentration and comparison with R2 Ferriscan. *J Cardiovasc Magn Reson* 1994; **16**: 40. doi: https://doi.org/10.1186/1532-429X-16-40
18. Henninger B, Zoller H, Rauch S, Finkenstedt A, Schocke M, Jaschke W, et al. R2* relaxometry for the quantification of hepatic iron overload: biopsy-based calibration and comparison with the literature. *Rofo* 2015; **187**: 472–9. doi: https://doi.org/10.1055/s-0034-1399318
19. Kühn JP, Hernando D, Muñoz del Rio A, Evert M, Kannengiesser S, Völzke H, et al. Effect of multipeak spectral modeling of fat for liver iron and fat quantification: correlation of biopsy with MR imaging results. *Radiology* 2012; **265**: 133–42. doi: https://doi.org/10.1148/radiol.12112520
20. Middleton MS, Heba ER, Hooker CA, Bashir MR, Fowler KJ, Sandrasegaran K, et al. Agreement between magnetic resonance imaging proton density fat fraction measurements and pathologist-assigned steatosis grades of liver biopsies from adults with nonalcoholic steatohepatitis. *Gastroenterology* 2017; **153**: 753–61. doi: https://doi.org/10.1053/j.gastro.2017.06.005
21. Noureddin M, Lam J, Peterson MR, Middleton M, Hamilton G, Le TA, et al. Utility of magnetic resonance imaging versus histology for quantifying changes in liver fat in nonalcoholic fatty liver disease trials. *Hepatology* 2013; **58**: 1930–40. doi: https://doi.org/10.1002/hep.26455
22. Tang A, Chen J, Le TA, Changchien C, Hamilton G, Middleton MS, et al. Cross-sectional and longitudinal evaluation of liver volume and total liver fat burden in adults with nonalcoholic steatohepatitis. *Abdom Imaging* 2015; **40**: 26–37. doi: https://doi.org/10.1007/s00261-014-0175-0
23. Srinivasa Babu A, Wells ML, Teytelboym OM, Mackey JE, Miller FH, Yeh BM, et al. Elastography in chronic liver disease: modalities, techniques, limitations, and future directions. *Radiographics* 2016; **736**: 1987–2006. doi: https://doi.org/10.1148/rg.2016160042
24. Schwenzer NF, Machann J, Haap MM, Martirosian P, Schraml C, Liebig G, et al. T2* relaxometry in liver, pancreas, and spleen in a healthy cohort of one hundred twenty-nine subjects-correlation with age, gender, and serum ferritin. *Invest Radiol* 2008; **43**: 854–60. doi: https://doi.org/10.1097/RLI.0b013e3181862413
25. Kühn JP, Meffert P, Heske C, Kromrey ML, Schmidt CO, Mensel B, et al. Prevalence of fatty liver disease and hepatic iron overload in a northeastern german population by using quantitative MR imaging. *Radiology* 2017; **284**: 706–16. doi: https://doi.org/10.1148/radiol.2017161228
26. Singh S, Venkatesh SK, Wang Z, Miller FH, Motosugi U, Low RN, et al. Diagnostic performance of magnetic resonance elastography in staging liver fibrosis: a systematic review and meta-analysis of individual participant data. *Clin Gastroenterol Hepatol* 2015; **13**: 440–51. doi: https://doi.org/10.1016/j.cgh.2014.09.046
27. Shi Y, Xia F, Li Q-ju, Li J-hui, Yu B, Li Y, et al. Magnetic resonance elastography for the evaluation of liver fibrosis in chronic hepatitis B and C by using both gradient-recalled echo and spin-echo echo planar imaging: a prospective study. *Am J Gastroenterol* 2016; **111**: 823–33. doi: https://doi.org/10.1038/ajg.2016.56
28. Singh S, Venkatesh SK, Loomba R, Wang Z, Sirlin C, Chen J, et al. Magnetic resonance elastography for staging liver fibrosis in non-alcoholic fatty liver disease: a diagnostic accuracy systematic review and individual participant data pooled analysis. *Eur Radiol* 2016; **26**: 1431–40. doi: https://doi.org/10.1007/s00330-015-3949-z
29. Huwart L, Salameh N, ter Beek L, Vicaut E, Peeters F, Sinkus R, et al. MR elastography of liver fibrosis: preliminary results comparing spin-echo and echo-planar imaging. *Eur Radiol* 2008; **18**: 2535–41. doi: https://doi.org/10.1007/s00330-008-1051-5

30. Trout AT, Serai S, Mahley AD, Wang H, Zhang Y, Zhang B, et al. Liver stiffness measurements with MR elastography: agreement and repeatability across imaging systems, field strengths, and pulse sequences. *Radiology* 2016; **281**: 793–804. doi: https://doi.org/10.1148/radiol.2016160209
31. Garteiser P, Sahebjavaher RS, Ter Beek LC, Salcudean S, Vilgrain V, Van Beers BE, et al. Rapid acquisition of multifrequency, multislice and multidirectional MR elastography data with a fractionally encoded gradient echo sequence. *NMR Biomed* 2013; **26**: 1326–35. doi: https://doi.org/10.1002/nbm.2958
32. Wang J, Glaser KJ, Zhang T, Shan Q, He B, Chen J, et al. Assessment of advanced hepatic MR elastography methods for susceptibility artifact suppression in clinical patients. *J Magn Reson Imaging* 2018; **47**: 976–87. doi: https://doi.org/10.1002/jmri.25818
33. Wagner M, Besa C, Bou Ayache J, Yasar TK, Bane O, Fung M, et al. Magnetic resonance elastography of the liver: qualitative and quantitative comparison of gradient echo and spin echo echoplanar imaging sequences. *Invest Radiol* 2016; **51**: 575–81. doi: https://doi.org/10.1097/RLI.0000000000000269
34. Wagner M, Corcuera-Solano I, Lo G, Esses S, Liao J, Besa C, et al. Technical failure of MR elastography examinations of the liver: experience from a large single-center study. *Radiology* 2017; **284**: 401–12. doi: https://doi.org/10.1148/radiol.2016160863
35. Kim YS, Song JS, Kannengiesser S, Seo SY. Comparison of spin-echo echoplanar imaging and gradient recalled echo-based MR elastography at 3 Tesla with and without gadoxetic acid administration. *Eur Radiol* 2017; **27**: 4120–8. doi: https://doi.org/10.1007/s00330-017-4781-4
36. Rump J, Klatt D, Braun J, Warmuth C, Sack I. Fractional encoding of harmonic motions in MR elastography. *Magn Reson Med* 2007; **57**: 388–95. doi: https://doi.org/10.1002/mrm.21152
37. Studholme C, Constable RT, Duncan JS. Accurate alignment of functional EPI data to anatomical MRI using a physics-based distortion model. *IEEE Trans Med Imaging* 2000; **19**: 1115–27. doi: https://doi.org/10.1109/42.896788